J. Synchrotron Rad. (1998). **5**, 817–819

Comparison of monochromators with a bent parabolic mirror and a varied-spacing grating for the 2.0 GeV high-brilliance synchrotron radiation source (VSX)

K. Mashima,[a]* N. Kihara[a] and E. Ishiguro[b]

[a]*Nikon Corporation, Shinagawa-ku, Tokyo 140, Japan, and* [b]*University of the Ryukyus, Nishihara-cho, Okinawa 903-01, Japan. E-mail: mashima@nikongw.nikon.co.jp*

(*Received 5 August 1997; accepted 15 December 1997*)

A design study of monochromators for a 2.0 GeV electron/positron storage ring for high-brilliance synchrotron radiation in the vacuum ultraviolet (VUV) and the soft X-ray regions is described. Two types of VUV/soft X-ray grazing-incidence monochromators, one with a bent parabolic mirror and the other with a varied-spacing grating, are designed. Without any slope error, the expected resolving power of the former is much higher, but the latter is less affected by slope errors of the optical elements.

Keywords: bent parabolic mirror monochromators; varied-spacing grating monochromators; VUV/soft X-ray monochromators.

1. Introduction

In designing a grazing-incidence monochromator with high resolution and high purity it is important to correct ray aberrations. For this purpose, various ideas have been proposed, such as employing the SX-700 monochromator (Petersen, 1982), which uses an elliptical mirror, or using a monochromator with a varied-spacing grating (Koike & Namioka, 1995). While it is not easy to manufacture aspherical mirrors by polishing, an alternative approach is to use bent mirrors (Ishiguro *et al.*, 1996). A simple wavelength-scanning mechanism is also important to achieve high performance.

Here, we report the design and performance of two types of monochromators: one using bent parabolic mirrors and equal-spacing plane gratings, and the other using spherical mirrors and varied-spacing plane gratings. Both monochromators have very simple mechanisms: fixed entrance and exit slits, and wavelength scanning only by grating rotation. Their design is described and a comparison of their performance is given.

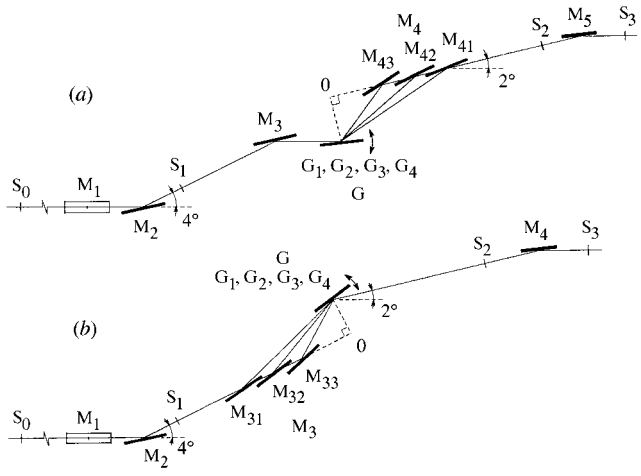

Figure 1
(*a*) Schematic diagram of the bent parabolic mirror monochromator. (*b*) Schematic diagram of the varied-spacing grating monochromator.

Table 1
Grating parameters and wavelength coverage.

The number of grooves is the value of the central position for the case of the varied-spacing gratings. K_g is a grating deviation angle: $\angle M_3GM_4/2$ for the bent parabolic mirror monochromator, or $\angle M_3GS_2/2$ for the varied-spacing grating monochromator.

Element	Length (mm)	No. of grooves per mm	K_g (°)	Wavelength region λ (Å)	Corresponding mirror
G_1	±70	1200	87	12–30	M_{41} M_{31}
G_2	±70	1200	85	25–100	M_{42} M_{32}
G_3	±70	400	85	90–280	M_{42} M_{32}
G_4	±70	400	80	250–1000	M_{43} M_{33}

2. Optics

2.1. *Bent parabolic mirror monochromator*

Fig. 1(*a*) is a schematic diagram of the monochromator, which consists of bent parabolic mirrors and equal-spacing plane gratings, where S_0 is an undulator source, and M_1 and M_2 are cylindrical or spherical mirrors. Rays with horizontal dispersion from S_0 are focused on the sample S_3 by M_1, and rays with vertical dispersion are focused on the entrance slit S_1 by M_2. The distances are S_0M_1 = 25 m, M_1M_2 = 1 m and M_2S_1 = 5.2 m. The deviation angles are $\angle S_0M_1M_2/2 = \angle M_1M_2S_1/2 = 88°$. The vertical magnification from S_0 to S_1 is 1/5.

M_3 is a bent parabolic mirror, collimating the rays with vertical dispersion from S_1 without aberration as S_1 is placed at the focal point of M_3. The deviation angle is $\angle S_1M_3G/2 = 88°$, and the distance S_1M_3 = 7 m. The equal-spacing plane gratings G_1–G_4 are interchangeable to cover the wavelength region. As they work with constant deviation-angle configuration, wavelength scanning is carried out only by grating rotation. The grating parameters are shown in Table 1. The bent parabolic mirrors M_{41}–M_{43}, which converge parallel rays on their foci without aberration, are also interchangeable to cover the wavelength region (see Table 1). The foci of these parabolic mirrors are fixed on the exit slit S_2, and consequently aberration-free monochromatic line images of S_1 are formed on S_2. The deviation angles are $\angle GM_{41}S_2/2 = 88°$, $\angle GM_{42}S_2/2 = 86°$ and $\angle GM_{43}S_2/2 = 81°$, and the distances are $M_{41}S_2$ = 1.484 m, $M_{42}S_2$ = 1.844 m, $M_{43}S_2$ = 2.046 m, OS_2 = 2.2 m and OG = 50 mm. A spherical mirror, M_5, converges the rays with vertical dispersion from S_2 on the sample S_3. Thus, a monochromatic small beam is formed on the sample S_3.

2.2. *Varied-spacing grating monochromator*

Fig. 1(*b*) is a schematic diagram of the monochromator, which consists of spherical mirrors and varied-spacing plane gratings. The elements from S_0 to S_1 are the same as those in Fig. 1(*a*). The spherical mirrors M_{31}–M_{33}, which convert vertically diverging rays from S_1 into vertically converging rays, are interchangeable to cover the wavelength region (see Table 1). The deviation

Table 2
Undulator source parameters.

σ_y is the r.m.s. source size and $\sigma_{y'}$ is the r.m.s. angular spread. Both values are for the vertical plane.

λ (Å)	σ_y (μm)	$\sigma_{y'}$ (μrad)	Grating
12	74.25	16.90	G_1
21	74.44	21.62	G_1
30	74.63	25.47	G_1
25	74.53	23.41	G_2
60	75.26	35.40	G_2
100	76.09	45.39	G_2
90	75.90	42.94	G_3
180	77.76	60.36	G_3
280	79.77	75.13	G_3
250	79.17	71.02	G_4
600	85.88	109.74	G_4
1000	92.96	141.58	G_4

angles are $\angle S_1M_{31}G/2 = 88°$, $\angle S_1M_{32}G/2 = 86°$ and $\angle S_1M_{33}G/2 = 81°$, and the distances are $S_1M_{31} = 7$ m, $S_1M_{32} = 7.359$ m, $S_1M_{33} = 7.561$ m, $S_1O = 7.715$ m, $GS_2 = 2.2$ m and $OG = 50$ mm. The varied-spacing plane gratings G_1–G_4 are interchangeable depending on the wavelength region (see Table 1). As they work with constant deviation-angle configuration, wavelength scanning is carried out only by grating rotation. Their spacing distributions were optimized with *Code-V* optical design software (Optical Research Associates) so that the vertical aberration between S_1 and S_2 is minimized. Consequently, monochromatic line images of S_1 are formed on the fixed-exit slit S_2. M_4 and S_3 are the same as M_5 and S_3, respectively, of Fig. 1(*a*).

3. Evaluation of the designed monochromators

The main purpose of this evaluation is to determine the resolving power of the designed monochromators with or without the slope errors of the optical elements. The resolving power was evaluated by means of ray tracing as described below.

3.1. *Undulator source and the source for ray tracing*

Table 2 gives the undulator source parameters of the 2.0 GeV high-brilliance synchrotron radiation that our calculation is based on. The vertical magnification from the source to the entrance slit is 1/5, so σ_y of Table 2 is reduced into $\sigma_y/5$ and $\sigma_{y'}$ is magnified to $5\sigma_{y'}$ at the entrance slit S_1. As the angular spread by diffraction of the entrance slit is $\sigma_{\rm diff} = \lambda/(4\pi\sigma_{\rm slit})$, where $\sigma_{\rm slit}$ is the half width of the entrance slit, the angular spread after the entrance slit becomes $\Sigma_{y'} = [(5\sigma_{y'})^2 + \sigma_{\rm diff}{}^2]^{1/2}$.

To achieve high resolving power we chose a 5 μm entrance-slit width ($\sigma_{\rm slit} = 2.5$ μm), which is about 1/3 of $\sigma_y/5$. The rays intercepted by the entrance slit do not contribute to the performance of the monochromators. Consequently, for ray tracing we assume an equivalent source on S_1 with constant illumination intensity (whose vertical width is 5 μm) and with a Gaussian angular distribution (whose vertical half width is $\Sigma_{y'}$). Ray tracing was carried out between S_1 and S_2, where the resolving power is determined, with several thousand rays that are generated randomly from S_1 with the probability distribution of the above-mentioned equivalent source (namely, a flat intensity and a Gaussian angular distribution). We also assume that the horizontal distribution of the source is uniform, because there is no horizontal optical power between S_1 and S_2.

3.2. *Ray tracing with slope errors*

Here, a slope error means a local angular deviation of the surface normal from the designed surface of the optical element. As mentioned above, the resolving power of the monochromators designed here is determined by the optical elements placed between S_1 and S_2. So, for ray tracing, slope errors are added only to the following elements: M_3, G_1–G_4 and M_{41}–M_{43} for the bent parabolic mirror monochromator, and M_{31}–M_{33} and G_1–G_4 for the varied-spacing grating monochromator. We assume that the slope error distribution is Gaussian: $f(\delta) \propto \exp(-\delta^2/2\sigma_s{}^2)$, where δ is a slope error. A ray, which is generated as described in §3.1, strikes some position of some element, and is then deflected by a slope error which is generated randomly with this probability distribution. Ray tracing with slope errors was carried out with $\sigma_s = 0.5$ μrad (0.1″), a value that we consider to be possible (Miura *et al.*, 1998). The slope errors were added to all elements at the same time.

4. Results

4.1. *Line profiles*

Fig. 2 shows examples of line profiles that were obtained from the vertical (dispersion direction) cross sections of the spot diagrams on the exit slit S_2 by the above-mentioned ray tracing, line profiles of the bent parabolic mirror monochromator without (*a*) and with (*b*) slope error, and of the varied-spacing grating monochromator without (*c*) and with (*d*) slope error. These profiles are at the same wavelength (λ = 180 Å) as the grating G_3 (see Table 1). The width of profile (*a*) is much smaller than that of (*c*). The long-tailed profile of (*c*) results from the remaining coma aberration of the varied-spacing grating monochromator. (The coma aberration is corrected at λ = 280 Å with grating G_3.) With $\sigma_s = 0.5$ μrad slope error, the profiles of both monochromators are spread out to almost the same width (Figs. 2*b* and 2*d*), but the long tails still remain in the profiles of the varied-spacing grating monochromator (Fig. 2*d*).

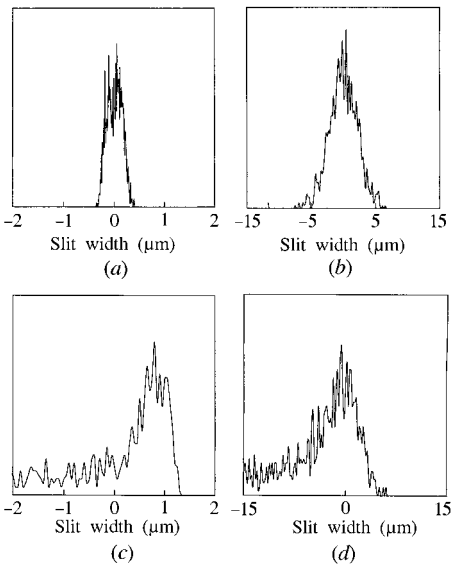

Figure 2
Line profiles of the bent parabolic mirror monochromator at λ = 180 Å with G_3, (*a*) without slope error and (*b*) with slope error $\sigma_s = 0.5$ μrad (0.1″). Line profiles of the varied-spacing grating monochromator at λ = 180 Å with G_3, (*c*) without slope error and (*d*) with slope error $\sigma_s = 0.5$ μrad (0.1″).

4.2. *Resolving power*

Some definitions of wavelength resolution $\Delta\lambda$ have already been given in Koike & Namioka (1995); here we simply define $\Delta\lambda$ as full width at the 1/e-maximum point of the line profile. Namely, $\Delta\lambda = W_e P\sin\beta/F$, where W_e is the full width at the 1/e-maximum point of the line profile, P, the pitch of the grating grooves, β, the diffraction angle from the grating surface, and F, the distance M_4S_2 for the bent parabolic mirror monochromator or the distance GS_2 for the varied-spacing grating monochromator. In both cases, the exit-slit width is regarded as zero.

Fig. 3(*a*) shows the resolving power $\lambda/\Delta\lambda$ of the bent parabolic mirror monochromator and Fig. 3(*b*) shows that of the varied-spacing grating; each depends on the wavelength region. Without the slope error, the resolving power of the former is much higher than that of the latter. However, with σ_s = 0.5 μrad slope error

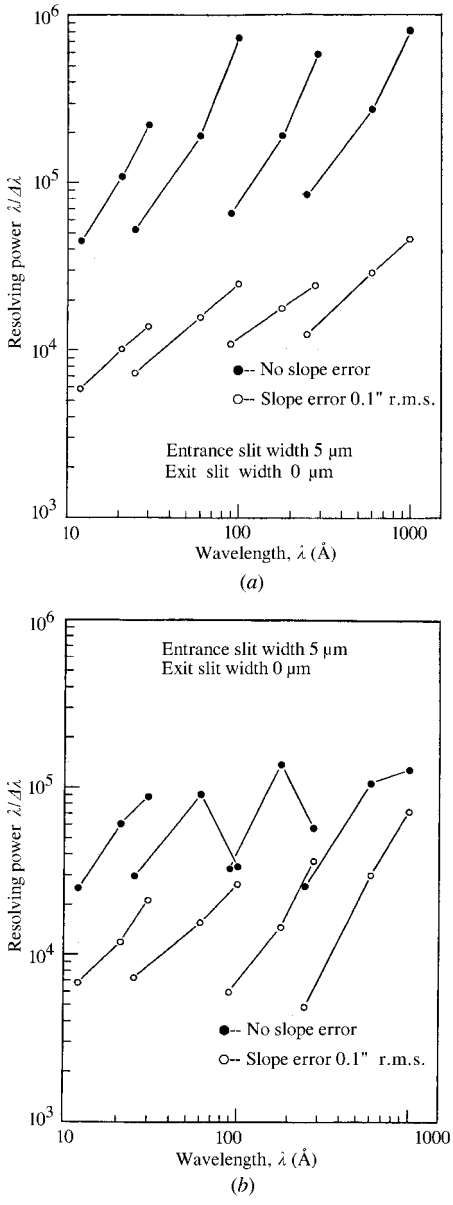

Figure 3
Resolving power $\lambda/\Delta\lambda$, with and without slope error, (*a*) of the bent parabolic mirror monochromator and (*b*) of the varied-spacing grating monochromator.

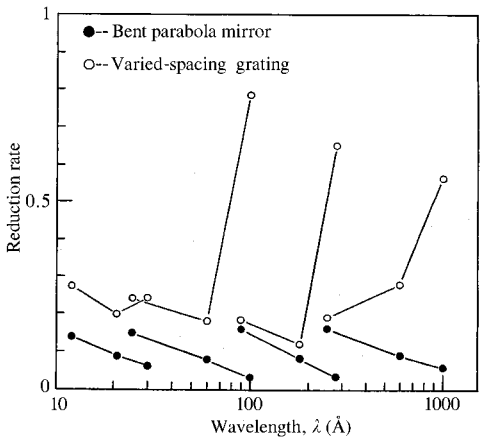

Figure 4
Reduction rate of the resolving power. This value is defined by [$(\lambda/\Delta\lambda)$ with slope errors]/[$(\lambda/\Delta\lambda)$ without slope errors].

the resolving power of both monochromators is reduced to almost the same value.

Fig. 4 shows the reduction rate of the resolving power, which is defined by [$(\lambda/\Delta\lambda)$ with slope errors]/[$(\lambda/\Delta\lambda)$ without slope errors]. This figure indicates that the degree of resolving power reduction of the varied-spacing grating monochromator is smaller than that of the bent parabolic mirror monochromator.

5. Discussion and conclusions

In Figs. 1(*a*) and 1(*b*), the incidence angle of G is α and the diffraction angle of G is β (both angles are from the grating surface), with the grating equation $\cos\alpha - \cos\beta = \lambda/P$, where P is a pitch of the grating grooves. When an incidence ray deviates by $d\alpha$, which is generated by a slope error $d\theta$ of M_3, the diffraction angle deviates $d\beta$, which is obtained by differentiating the grating equation $d\beta = (\sin\alpha/\sin\beta)\,d\alpha = (\sin\alpha/\sin\beta)2d\theta$. In the case of $\alpha < \beta$ (this design), the ray deviation by slope errors of M_3 is reduced through the grating. On the other hand, the ray deviation by slope errors of M_4 is $2d\theta$. The slope error effect of a mirror placed before the grating is smaller than that of a mirror placed after the grating. Consequently, in this design, the varied-spacing grating monochromator is less affected by slope errors of the optical elements, as shown in Fig. 4.

The bent parabolic mirror monochromator, which employs aberration-free optics, has higher resolving power, but is more affected by slope errors. As a result, the slope error reduces the resolving power of both monochromators to almost the same value. However, the wavelength purity of the varied-spacing grating monochromator should be worse because of the long tails of the line profiles.

The bent parabolic mirror monochromator has the potential to achieve much higher resolving power as the manufacturing precision of the optical elements is improved in the future.

References

Ishiguro, E., Sugawara, H., Okuyama, M., Waku, N., Sato, S. & Takigawa, T. (1996). *J. Electron Spectrosc. Relat. Phenom.* **80**, 489–492.
Koike, M. & Namioka, T. (1995). *Rev. Sci. Instrum.* **66**, 2144–2146.
Miura, S., Kihara, N., Mashima, K., Miyaji, A., Wakamiya, K., Shiozawa, H., Fukuda, Y. & Ichikawa, H. (1998). *J. Synchrotron Rad.* **5**, 808–810.
Petersen, H. (1982). *Opt. Commun.* **40**, 402–406.